Chapter 6

Ferro Fluid Lubrication of a Rough Porous Secant Slider – A Study of Shliomis model

This chapter aims to study the squeeze film behaviour for a Shliomis model based magnetic fluid lubrication of a rough porous secant slider. To evaluate the effect of transverse surface roughness, the model of Christensen and Tonder is adopted. The associated stochastically averaged Reynolds type equation is solved to obtain the pressure distribution leading to the calculation of load carrying capacity. The graphical results indicate that the adverse effect of surface roughness can be reduced to a large extent by the ferro-fluid lubrication. Further, Shliomis model proves to be superior to the Neuringer-Rosensweig model, here.

6.1 Introduction

Lubrication in bearings is well known in industrial applications and their main advantages compared with rolling and friction bearings, are their role in reduction of friction and resulting in very high precision. Various applications and the investigations of the rheological properties of magnetic fluids gained noticeable importance during the last few years.The application of magnetic fluid as a lubricant was studied by a number of authors [Agrawal (1986), Bhat and Deheri (1995), Urreta et al. (2009), Huang et al. (2011)]. In all these studies it has been noticed that the performance of the bearing system could be enhanced by using a magnetic fluid as the lubricant.

Shliomis (1972) developed a ferrofluid flow model, in which the effects of rotation of magnetic particles, their magnetic moments and the volume concentration were included. Singh and Gupta (2012) theoretically investigated the effect of ferrofluid on the dynamic characteristics of curved slider bearings using Shliomis model, on the ground of the ferrohydrodynamic model proposed by Shliomis (1972). It was established from the above studies that the volume concentration and the intensity of magnetic field provided an increase in the load carrying capacity and the time of approach. Surface roughness evaluation is very essential for many fundamental problems such as friction, load carrying capacity, contact deformation, heat and electric current conditions, tightness of contact joints and positional accuracy. Tzeng and Seibel (1967) realized the random nature of roughness orientation and developed a stochastic method to describe the surface roughness. Later on, this was modified by Christensen and Tonder (1969a, 1969b, 1970) to propose a more general method for analyzing the effect of both the roughness patterns (transverse as well as longitudinal). This method was adopted by many investigators [Gupta and Deheri (1996), Deheri and Patel (2011), Patel and Deheri (2012), Patel et. al. (2012)]. Patel and Deheri (2014 a) analyzed the effect of Shliomis model based ferrofluid lubrication on the squeeze film between curved rough annular plates with comparison between two different porous structures. Kozeny-Carman's formulation and Irmay's model were treated for porous structures. It was noticed that the effect of morphology parameter and volume concentration parameter increased the load carrying capacity of the bearing system. Patel and Deheri (2014 d) dealt with the effect of different porous structures on the performance of a Shliomis model based magnetic squeeze film in rotating rough porous curved circular plates. It was seen that the adverse effect of transverse roughness could be compensated by the positive effect of magnetization in the case of negatively skewed roughness, suitably choosing the rotation ratio and the curvature parameters. Shah and Bhat (2003 b) analyzed a bearing with a secant shaped slider and with the stator having a porous facing backed by a solid wall using a magnetic fluid lubricant flowing as per Jenkins model. It was observed that the load carrying capacity decreased and friction as well as the coefficient of friction increased with increasing values of the material parameter. Shukla and Deheri (2011) dealt with the performance of a porous rough secant shaped slider bearing under the presence of a magnetic fluid lubricant. It was noticed that the negative effect of porosity and standard deviation could be reduced to a large extent by the positive effect of the magnetization parameter, in the case of negatively skewed roughness. Patel and Deheri (2015) presented an analytical solution for the performance

characteristics of a magnetic fluid based double layered porous rough slider bearing. It was revealed that the increased load carrying capacity owing to double layered got enhanced due to the magnetic fluid lubricant and this went a long way in reducing the adverse effect of roughness in the case of Kozeny-Carman model. Patel et. al. (2015) studied that the performance of an idealized rough porous hydrodynamic plane slider bearing. It was concluded that the transverse surface roughness induced an adverse effect on the performance of bearing due to the negative effect of porosity. However, the situation was relatively better in the case of negatively skewed roughness.

6.2 Analysis

The configuration of plate slider bearing with squeeze velocity $\dot{h} = dh/dt$ is displayed in Figure 6.1. The lower surface is a slider of length A and moving with uniform velocity U in the x direction. Also, the slider is having width B in the y direction with $A \ll B$. Moreover, h_2 and h_1 are maximum and minimum film thicknesses respectively.

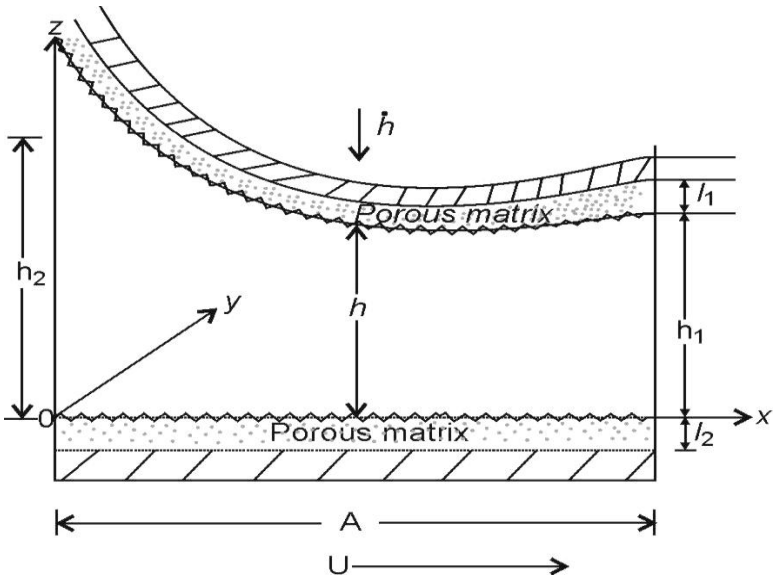

Fig. 6.1 Configuration of the bearing system

The bearing surfaces are considered to be transversely rough. The stochastic modelling of surface roughness by Christensen and Tonder (1969 a, 1969 b, 1970) for roughness aspects is discussed in Chapter 4 in detail.

The basic equations governing Shliomis model based Ferro-fluid lubrication are (Shliomis (1972))

$$-\nabla p+\eta\nabla^2\bar{q}+\mu_0\left(\overline{M}\nabla\right)\overline{H}+\frac{1}{2\tau_s}\nabla\times\left(\bar{S}-I\overline{\Omega}\right)=0 \tag{6.1}$$

$$\overline{\Omega}=\frac{1}{2}\nabla\times\bar{q} \tag{6.2}$$

$$\bar{S}=I\overline{\Omega}+\mu_0\tau_s\left(\overline{M}\times\overline{H}\right) \tag{6.3}$$

$$\overline{M}=M_0\frac{\overline{H}}{H}+\frac{\tau_B}{I}\left(\bar{S}\times\overline{M}\right) \tag{6.4}$$

$$\nabla\times\overline{H}=0 \tag{6.5}$$

and

$$\nabla\left(\overline{H}+\overline{M}\right)=0 \tag{6.6}$$

where p represents the pressure, η is the viscosity of the suspension, μ_0 denotes the permeability of free space, $\overline{H}$ is the applied magnetic field, $\overline{M}$ is the magnetization vector, $\bar{q}$ denotes the fluid velocity, $\bar{S}$ represents internal angular momentum, I is the sum of moments of inertia of the particle per unit volume, τ_B is the Brownian relaxation time, τ_s is the magnetic moments relaxation time and M_0 denotes the equilibrium magnetization.

Combining all above equations, one can get

$$-\nabla p+\eta\nabla^2\bar{q}+\mu_0\left(\overline{M}\nabla\right)\overline{H}+\frac{1}{2}\mu_0\nabla\times\left(\overline{M}\times\overline{H}\right)=0 \tag{6.7}$$

and

$$\overline{M}=M_0\frac{\overline{H}}{H}+\tau_B\overline{\Omega}\times\overline{M}-\frac{\mu_0\tau_B\tau_s}{I}\overline{M}\times\left(\overline{M}\times\overline{H}\right) \tag{6.8}$$

For the strong magnetic field Langevin's parameter $\xi>1$, the above equation takes the form,

$$\overline{M}=\frac{M_0}{H}\left[\overline{H}+\bar{\tau}\left(\overline{\Omega}\times\overline{H}\right)\right] \tag{6.9}$$

with

$$\bar{\tau}=\frac{6\eta\varphi}{nk_BT\left(1+\xi\coth\xi\right)} \tag{6.10}$$

where

$$M_0 = n\mu\left(\coth\xi - \frac{1}{\xi}\right), H = \frac{k_B T\xi}{\mu_0\mu}, \tag{6.11}$$

for a suspension of spherical particles

$$\frac{I}{\tau_s} = 6\eta\varphi \quad \text{and}\ \tau_B = \frac{3\eta V}{k_B T}, \tag{6.12}$$

$\varphi = nV$ is the volume concentration of the particles, k_B is the Boltzmann constant, n denotes the number of particles per unit volume, V is the volume of the particle, T represents the temperature and μ is the magnetic moment of a particle.

Under the uniform magnetic field $\overline{H} = (0,0,H_0)$, equations (6.7-6.9) yield

$$\frac{\partial^2 u}{\partial z^2} = \frac{1}{\eta(1+\tau)}\frac{dp}{dx} \tag{6.13}$$

where

$$\tau = \frac{3}{2}\varphi\frac{\xi - \tanh\xi}{\xi + \tanh\xi} \tag{6.14}$$

Solving equation (6.13) under the no slip boundary conditions

$$u = 0 \text{ at } z = h \text{ and } u = U \text{ at } z = 0,$$

one can find

$$u = \frac{1}{\eta(1+\tau)}\left(\frac{z^2}{2} - \frac{h}{2}z\right)\frac{\partial p}{\partial x} + U\left(1 - \frac{z}{h}\right) \tag{6.15}$$

Substituting u in the integral form of the continuity equation for the film region

$$\frac{\partial}{\partial x}\int_0^h u dz + w_h - w_0 = 0 \tag{6.16}$$

yields

$$\frac{d}{dx}\left[-\frac{h^3}{12\eta(1+\tau)}\frac{dp}{dx} + \frac{Uh}{2}\right] = \dot{h} \tag{6.17}$$

considering

$$w_h = -\dot{h} \text{ and } w_h = -\dot{h}\ w_0 = 0$$

as the lower plate is impermeable.

If η_0 represents the viscosity of the main liquid, the viscosity of the suspension is given by the Einstein formula (Shliomis (1972))

$$\eta = \eta_0\left(1+\frac{5}{2}\varphi\right) \tag{6.18}$$

Equations (6.18) and (6.19) lead to

$$\frac{d}{dx}\left[-\frac{h^3}{12\eta_0\left(1+\frac{5}{2}\varphi\right)(1+\tau)}\frac{dp}{dx}+\frac{Uh}{2}\right]=\dot{h} \tag{6.19}$$

The usual assumptions of hydromagnetic lubrication [Bhat (2003), Prajapati (1995), Patel and Deheri (2011 a), Deheri et al. (2005)] are made. Now, the often used well-known stochastic averaging method of Christensen and Tonder (1969 a, 1969 b and 1970) transforms equation (6.19) to the modified Reynolds equation governing the pressure distribution:

$$\frac{d}{dx}\left[-\frac{g(h)}{12\eta_0\left(1+\frac{5}{2}\varphi\right)(1+\tau)}\frac{dp}{dx}+\frac{U\{g(h)\}^{\frac{1}{3}}}{2}\right]=\dot{h} \tag{6.20}$$

where ,

$$g(h)=h^3+3h^2\alpha+3\left(\alpha^2+\sigma^2\right)h+3\sigma^2\alpha+\alpha^3+\varepsilon+12\phi H$$

Introducing the non-dimensional quantities,

$$X=\frac{x}{A},\bar{h}=\frac{h}{h_2}=sec\left(\frac{\pi(1-X)}{2}\right)$$

$$P=\frac{h_2^2 p}{U\eta_0 A},D=\frac{A\dot{h}}{Uh_2},\bar{\sigma}=\frac{\sigma}{h_2},\bar{\alpha}=\frac{\alpha}{h_2},$$

$$\bar{\varepsilon}=\frac{\varepsilon}{h_2^3},\psi=\frac{\phi H}{h_2^3} \tag{6.21}$$

and solving above equation subject to the boundary conditions

$$P(0)=P(1)=0 \tag{6.22}$$

One arrives at the dimensionless pressure as

$$P=\int_0^X\frac{F}{G}dX-D\int_0^X\frac{X}{G}dX-Q\int_0^X\frac{1}{G}dX \tag{6.23}$$

where

$$G=\frac{g\left(\bar{h}\right)}{E},\qquad E=12\left(1+\frac{5}{2}\varphi\right)\left(1+\tau\right),\qquad F=\frac{g\left(\bar{h}\right)^{\frac{1}{3}}}{2}\qquad Q=\frac{\int_0^1\frac{F}{G}dX-D\int_0^1\frac{X}{G}dX}{\int_0^1\frac{1}{G}dX}$$

and

$$g(\bar{h})=\bar{h}^3+3\bar{h}^2\bar{\alpha}+3\left(\bar{\alpha}^2+\bar{\sigma}^2\right)\bar{h}+3\bar{\sigma}^2\bar{\alpha}+\bar{\alpha}^3+\bar{\varepsilon}+12\psi$$

The non dimensional load carrying capacity then can be obtained as

$$W=\frac{h_2^2w}{BUA^2\eta_0}$$

$$=\int_0^1\frac{F}{G}\left(1-X\right)dX-D\int_0^1\frac{X}{G}\left(1-X\right)dX-Q\int_0^1\frac{1}{G}\left(1-X\right)dX \qquad (6.24)$$

6.3 Results and Discussion

As can be seen, the magnetization increases the viscosity of the lubricants which causes increased pressure and hence load carrying capacity. Further, for smooth bearing system, this discussion results in the investigation presented in Bhat (2003). A comparison of the present results with that of Bhat (2003) shows that Shliomis model is better than Neuringer-Rosensweig model

The variation of load carrying capacity with respect to the magnetization parameter τ presented in figures 6.2-6.5 indicates that the load carrying capacity increases sharply with increasing magnetization. Further, the effect of skewness on the distribution of load carrying capacity with respect to magnetization is marginal. Also, the initial combined effect of porosity and standard deviation on the load carrying capacity remains nominal.

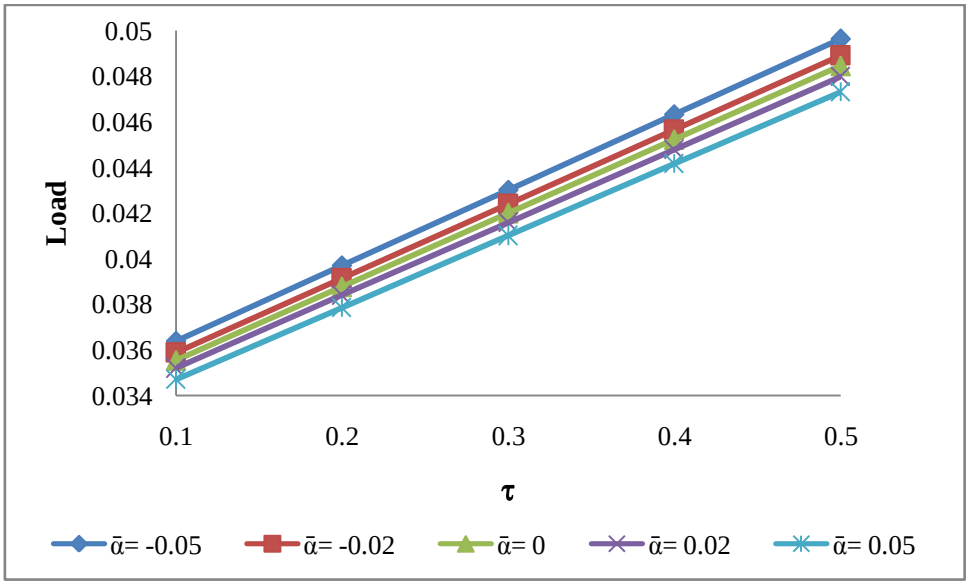

Fig. 6.2 : Variation of Load carrying capacity with respect to τ and $\bar{\alpha}$

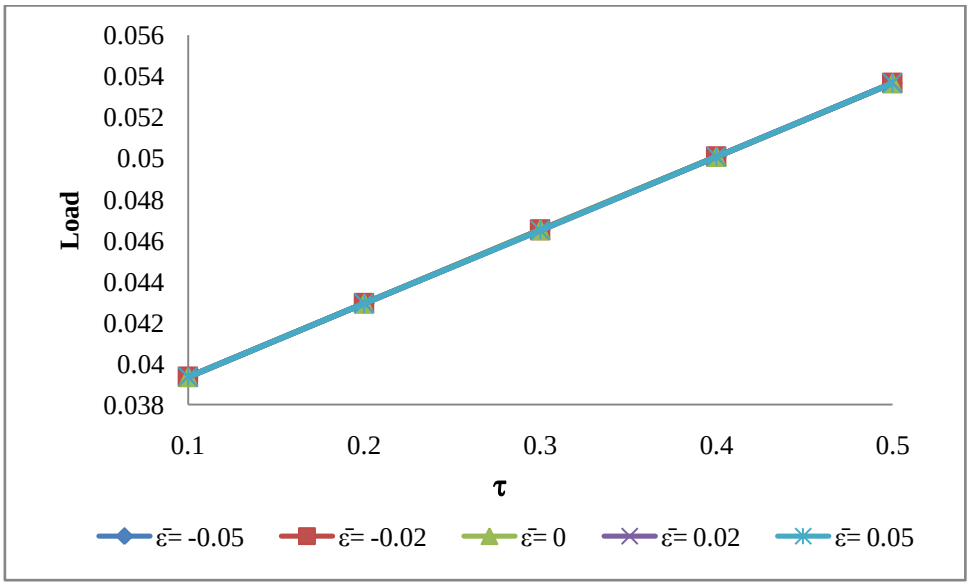

Fig. 6.3 : Variation of Load carrying capacity with respect to τ and $\bar{\varepsilon}$

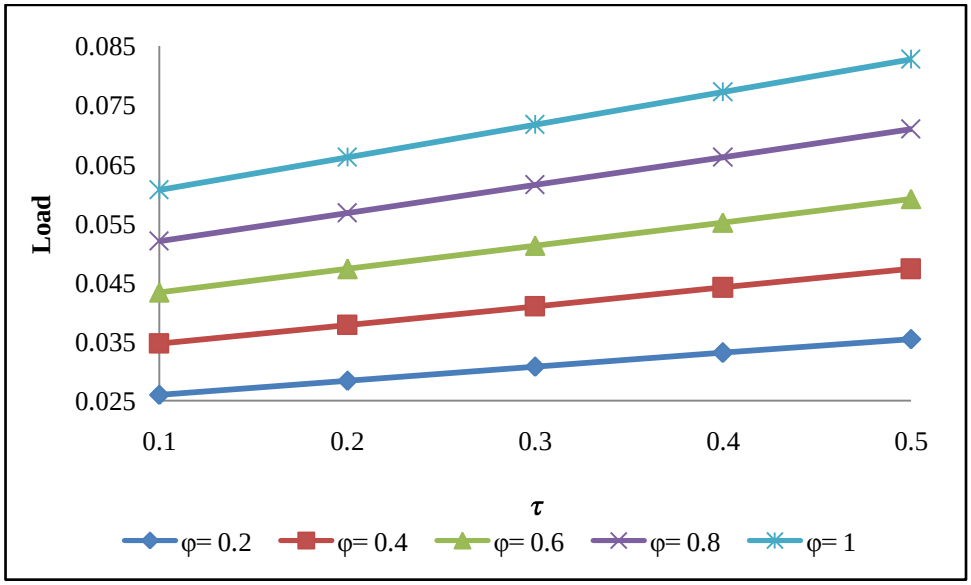

Fig. 6.4 : Variation of Load carrying capacity with respect to τ and φ

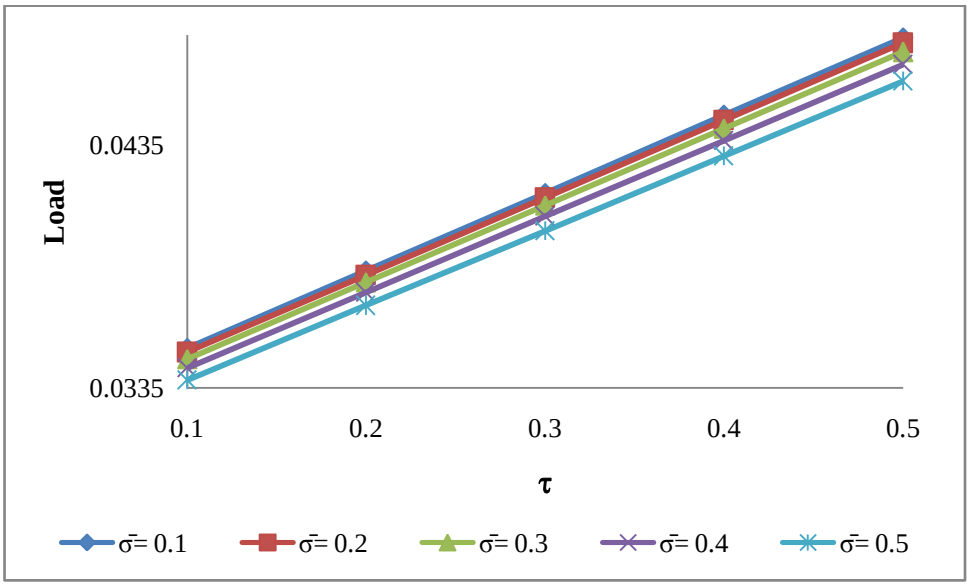

Fig. 6.5 : Variation of Load carrying capacity with respect to τ and $\bar{\sigma}$

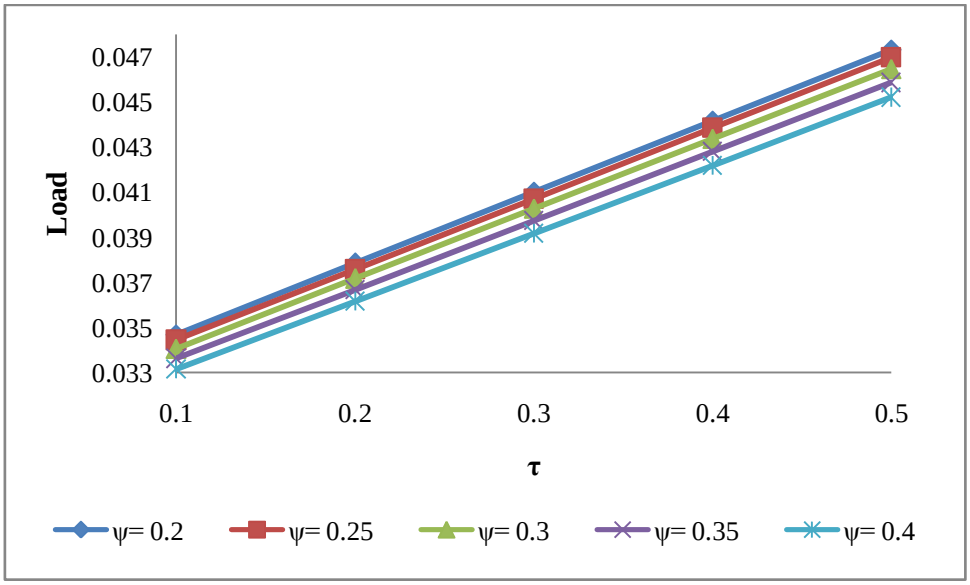

Fig. 6.6 : Variation of Load carrying capacity with respect to τ and ψ

Figures 6.7-6.10 dealing with the variation of load carrying capacity with respect to $\bar{\sigma}$ make it clear that the load carrying capacity falls sharply except in the case of φ where the fall is all most negligible. Further, the effect of skewness on the load carrying capacity remains almost negligible with respect to $\bar{\sigma}$

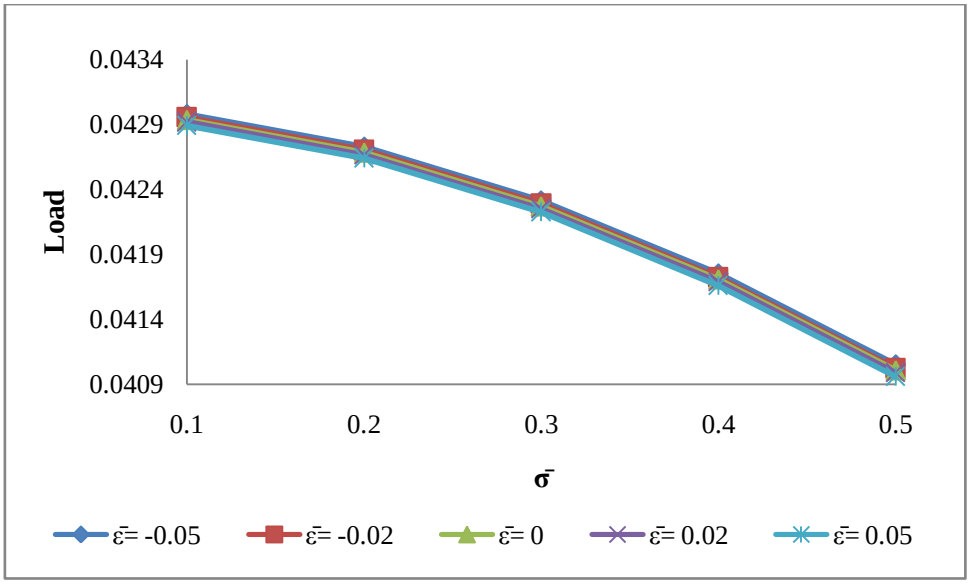

Fig. 6.7 : Variation of Load carrying capacity with respect to $\bar{\sigma}$ and $\bar{\varepsilon}$

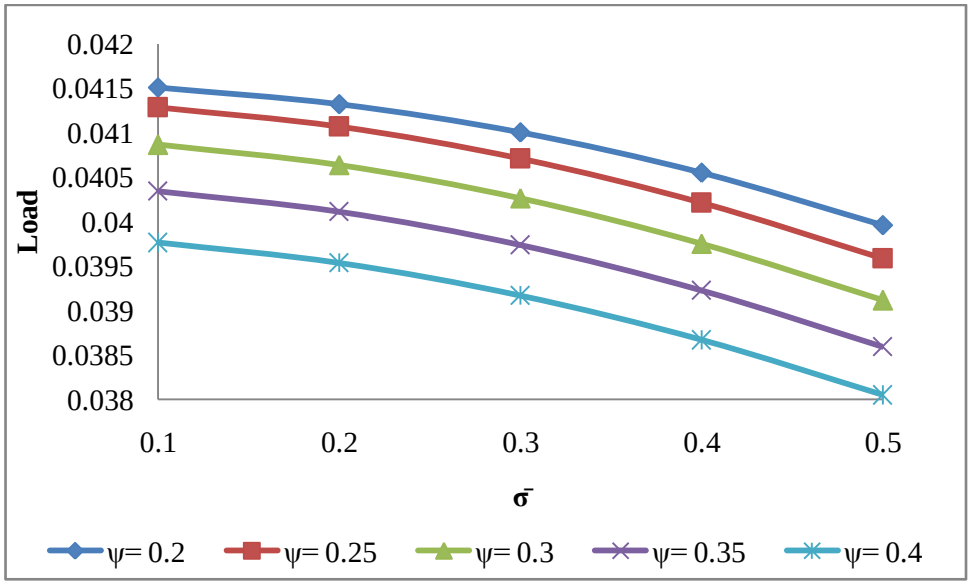

Fig. 6.8 : Variation of Load carrying capacity with respect to $\bar{\sigma}$ and ψ

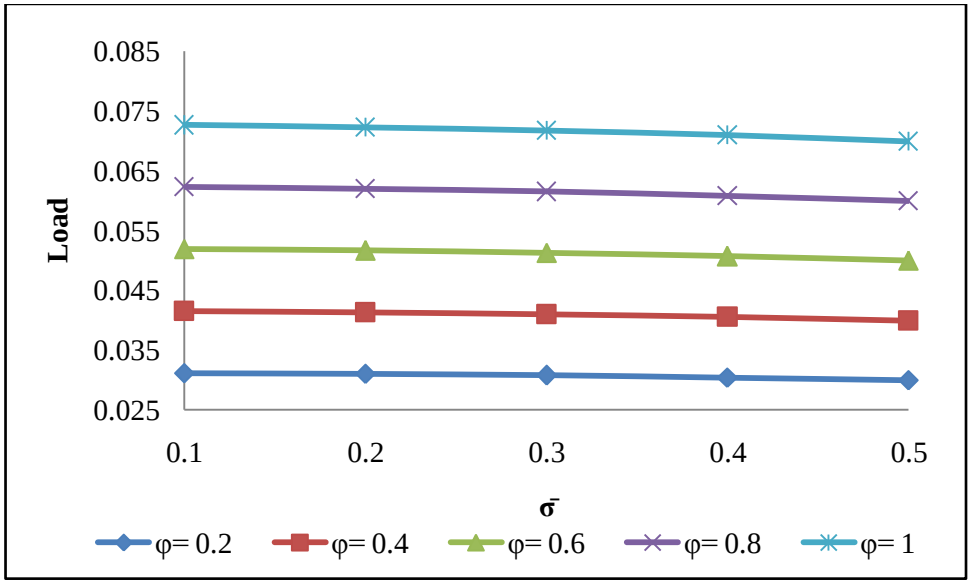

Fig. 6.9 : Variation of Load carrying capacity with respect to $\bar{\sigma}$ and φ

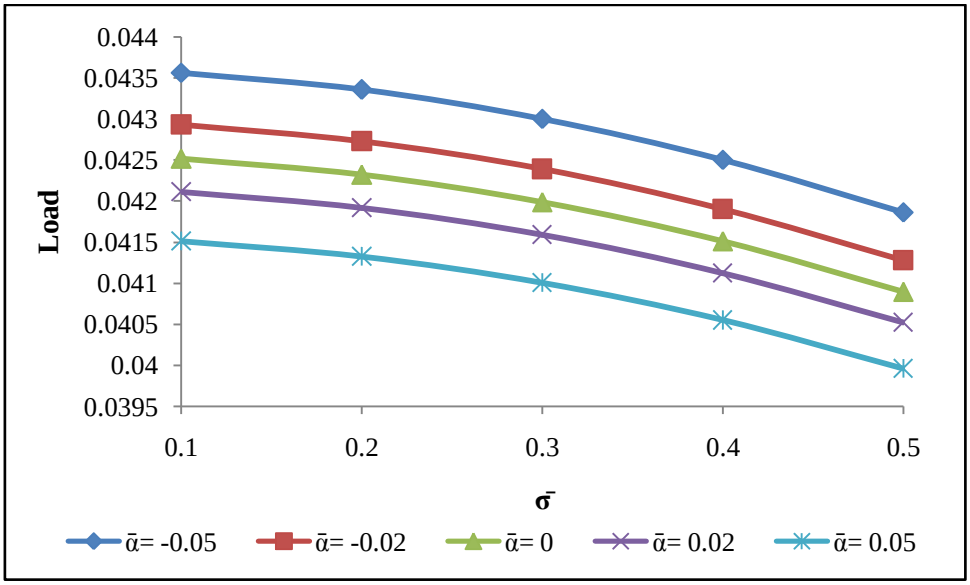

Fig. 6.10 : Variation of Load carrying capacity with respect to $\bar{\sigma}$ and $\bar{\alpha}$

The effect of variance shown in figures 6.11-6.13 establish that the positive variance decreases the load carrying capacity, while the load carrying capacity increases with variance (–ve). It is observed that skewness follows the path of variance so far as the trends of load carrying capacity are concerned. In other words the positive effect of variance (–ve) gets enhanced due to the negatively skewed roughness.

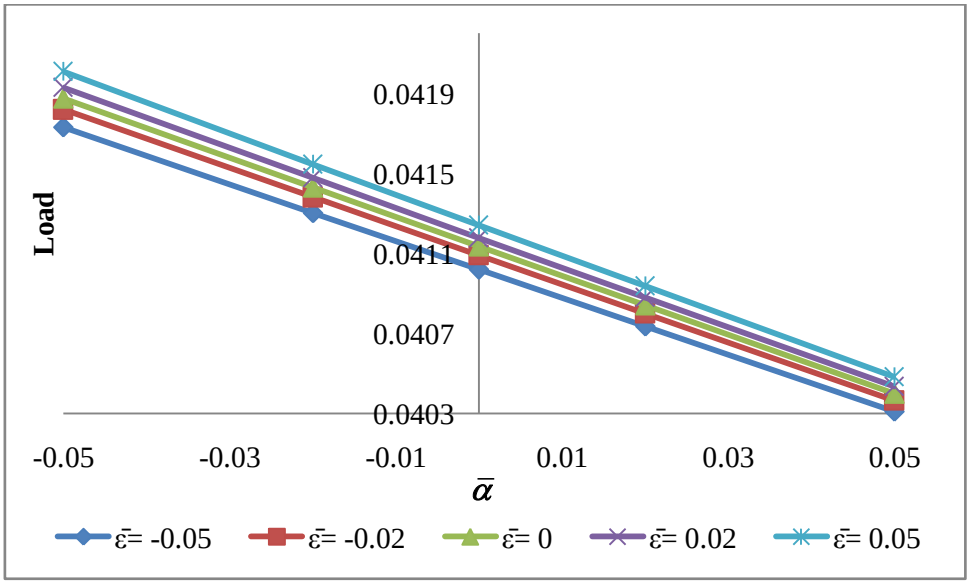

Fig. 6.11: Variation of Load carrying capacity with respect to $\bar{\alpha}$ and $\bar{\varepsilon}$.

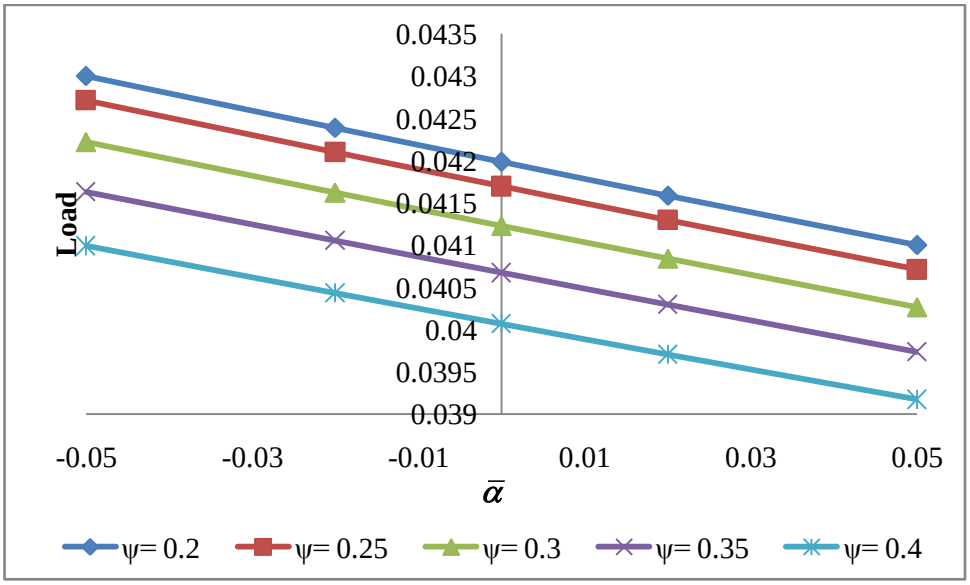

Fig. 6.12 : Variation of Load carrying capacity with respect to $\bar{\alpha}$ and ψ

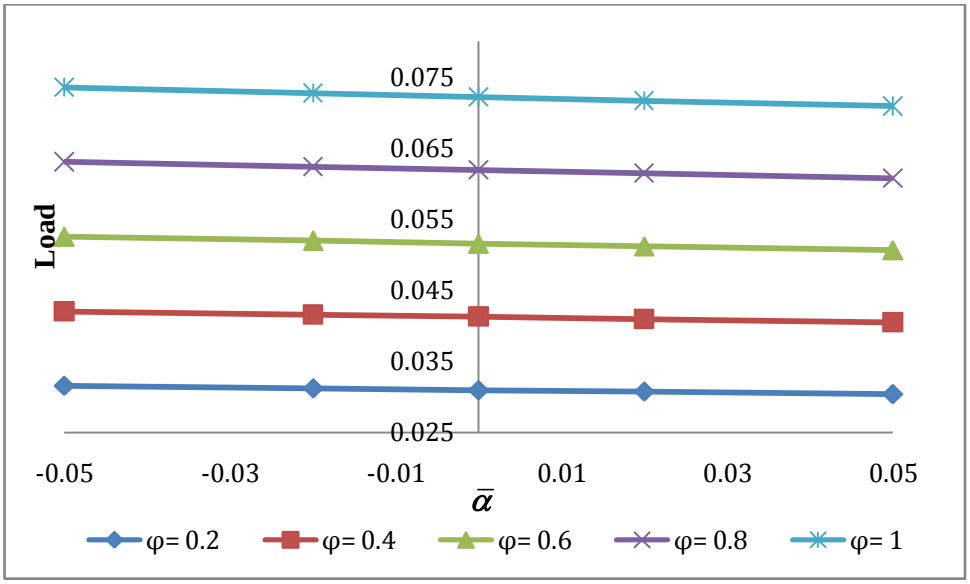

Fig. 6.13 : Variation of Load carrying capacity with respect to $\bar{\alpha}$ and φ

Lastly, the fact that the load carrying capacity increases with the increase in the volume concentration parameter φ, is provided in figures 6.14-6.16. Here also, the effect of skewness on the load carrying capacity with respect to volume concentration parameter, is nominal.

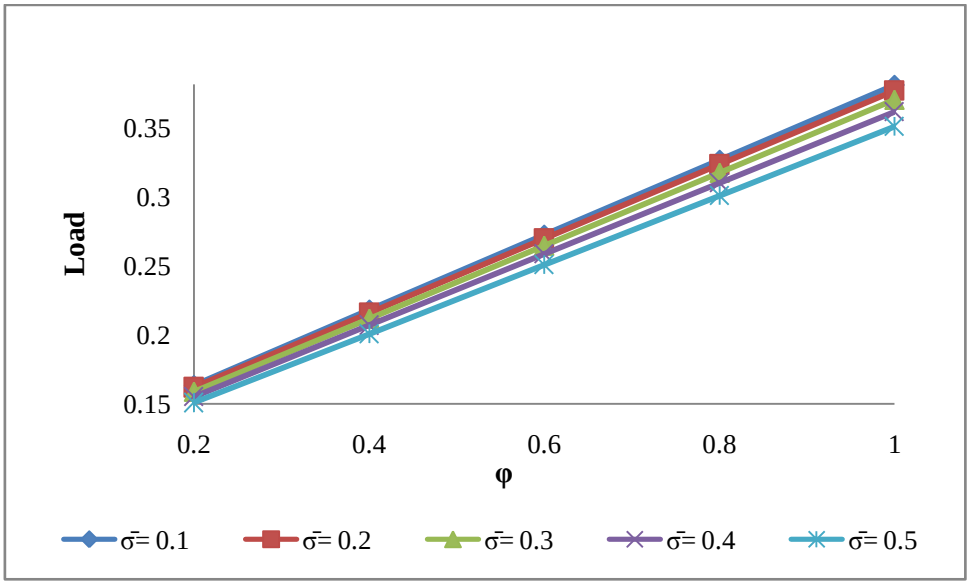

Fig. 6.14 : Variation of Load carrying capacity with respect to φ and $\bar{\sigma}$

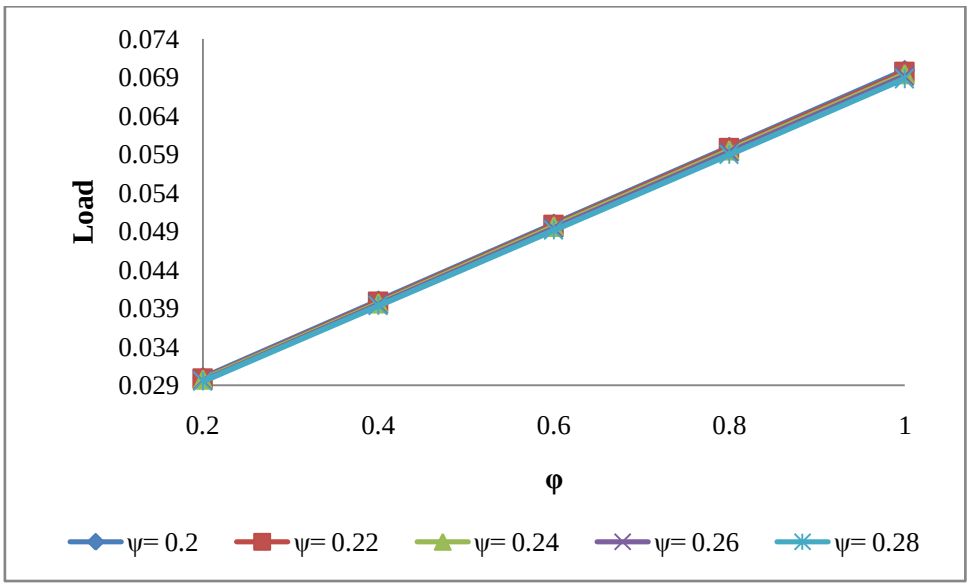

Fig. 6.15 : Variation of Load carrying capacity with respect to φ and ψ

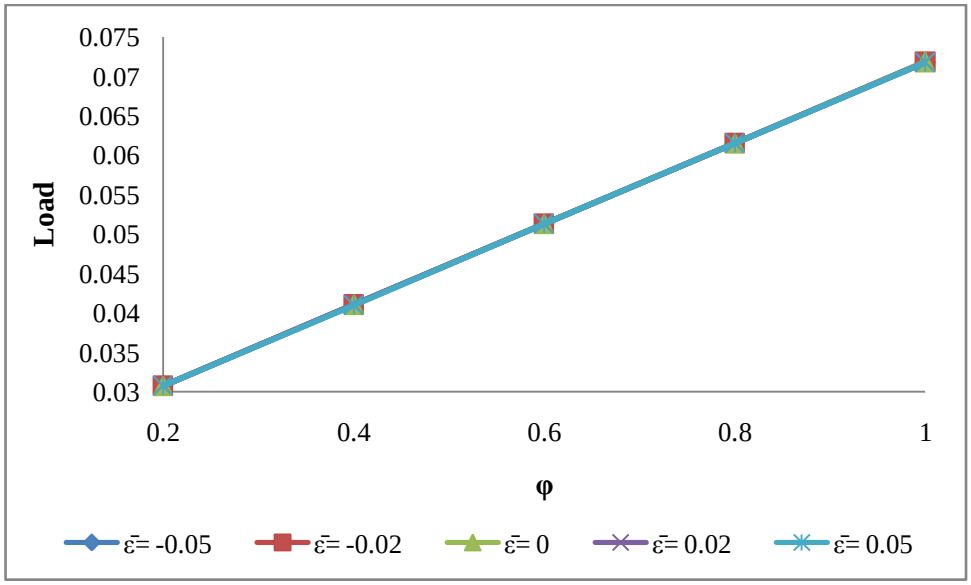

Fig. 6.16 : Variation of Load carrying capacity with respect to φ and $\bar{\varepsilon}$

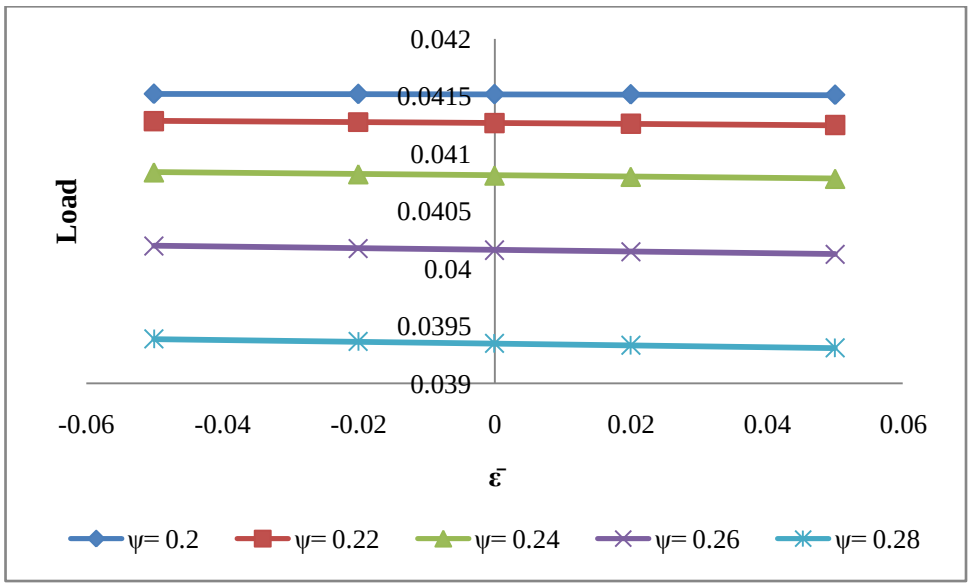

Fig. 6.17 : Variation of Load carrying capacity with respect to $\bar{\varepsilon}$ and ψ

This adverse effect of roughness may be due to the fact that the motion of the lubricant gets opposed by roughness, resulting in lowering of pressure and hence the load. As usually observed, the load carrying capacity gets decreased due to the porosity, as some amount of lubricant enters into the pores, which can be seen in Fig. 6.17.

It is revealed that the effect of variance is more crucial as compared to skewness. This study offers the suggestions that the combined positive effect of variance (-ve) and negatively skewed roughness may be channelized for improving the bearing performance.

6.4 Validation

Table 6.1

	Load Carrying Capacity (calculated for $\bar{\sigma}$=0.01, $\bar{\alpha}$= -0.05, $\bar{\varepsilon}$= -0.05, τ=0.3)		
ψ =	**with Rough Porous surface as in this chapter**	**with Smooth porous surface by Shah and Parikh (2014)***	**increase in %**
0.0001	0.033444372	0.027740936	20.56
0.0005	0.033521651	0.027871996	20.27
0.001	0.033617305	0.028033983	19.92
0.005	0.034346296	0.029260052	17.38
0.01	0.035174022	0.030634442	14.82

Table 6.2

	Load Carrying Capacity (calculated for $\bar{\sigma}$=0.01, $\bar{\alpha}$= -0.05, $\bar{\varepsilon}$= -0.05, ψ=0.001)		
τ =	**with Rough Porous surface as in this chapter**	**with Smooth porous surface by Shah and Parikh (2014)***	**increase in %**
0.1	0.028445412	0.023721062	19.92
0.2	0.031031358	0.025877522	19.92
0.3	0.033617305	0.028033983	19.92
0.4	0.036203252	0.030190443	19.92
0.5	0.038789198	0.032346903	19.92

From Table-6.1 & 6.2, we can say that better performs is given by the bearing system due to rough porous surface as compared to bearing system with smooth porous surface studied by Shah and Parikh (2014).

6.5 Conclusion

In the existing research Shliomis model based Ferro-fluid lubrication of a porous secant pad slider bearing is discussed. Also, it is well known that the roughness affects the bearing system significantly. One gets the information from the literature regarding Ferro-fluid flow that, Shliomis model registers an improved performance as compared to Neuringer-Rosensweig model. This investigation indicates that the adverse effect of transverse surface roughness can be overcome by a suitable magnetic strength. However, from the bearings life period point of view the roughness aspects must be addressed while designing the bearing system.